J Mater Sci (2015) 50:1783–1793
DOI 10.1007/s10853-014-8741-y

Role of different factors in the glass-forming ability of binary alloys

D. V. Louzguine-Luzgin · N. Chen · A. Yu. Churymov · L. V. Louzguina-Luzgina · V. I. Polkin · L. Battezzati · A. R. Yavari

Received: 5 October 2014 / Accepted: 22 November 2014 / Published online: 9 December 2014

Abstract In the present work, we discuss the glass-forming ability of various binary alloys in which the glassy phase was not formed even by melt spinning technique with high cooling rate of the melt up to 1 MK/s (some consisted of partly glassy phase), though by commonly accepted guidelines, these alloys could be as good glass-formers as many other binary glasses. The alloys studied belong to binary systems with multiple eutectics; the constituent elements have a negative enthalpy of mixing, and a significant variability of atomic size differences is observed from system to system. The results indicate the necessity of taking into account simultaneously various factors influencing the glass-forming ability including melt fragility.

D. V. Louzguine-Luzgin (✉) · A. R. Yavari
WPI Advanced Institute for Materials Research, Tohoku University, Aoba-Ku, Sendai 980-8577, Japan
e-mail: dml@wpi-aimr.tohoku.ac.jp

N. Chen
School of Materials Science and Engineering, Tsinghua University, Beijing 100084, People's Republic of China

A. Yu. Churymov · L. V. Louzguina-Luzgina · V. I. Polkin
National University of Science and Technology "MISiS", Moscow 119049, Russia

L. Battezzati
Dipartimento di Chimica, IFM Università di Torino, Turin, Italy

A. R. Yavari
SIMAP-CNRS, Institut Polytechnique de Grenoble, BP 75, St-Martin-d'Hères Campus, 38402 Saint-Martin-d'Hères, France

Introduction

Metallic glasses and bulk metallic glasses (BMG) are being extensively studied at present [1–5]. On solidification of the melt, they are typically formed either in the shape of 10^1–10^2 μm thick ribbons by rapid solidification onto a rotating Cu wheel [2] or in bulk shape of 10^0–10^2 mm thick rods by Cu mold casting [6]. The cooling rate of the melt spinning technique attains 1 MK/s. Even upon Cu mold casting of BMGs having several millimeters in diameter, the cooling rate reaches tens, hundreds, and even thousands Kelvin per second depending on the mold cavity size and melt temperature [7].

According to the principles and rules postulated by Inoue, there are three most important factors influencing bulk glass formation: number of alloy components (chemical elements), large atomic size difference, and large negative mixing enthalpy among the constituent elements. All of them represent indispensable conditions in order to form bulk glassy alloys leading to good glass-forming ability (GFA) [1, 8] and relatively high thermal stability against crystallization [9].

First principle (the number of components) leads to the formation of dense-packed structures, "deep" ternary and quaternary eutectics (together with large difference in electronegativity [10]) as well as leads to elemental "confusion" on solidification [2]. Recently good correlation was found between the alloy system complexity (number of alloying elements) and critical diameter of the glassy sample [8]. Role of the second principle (atomic size ratio) has been rationalized by Egami and Waseda [11, 12] who investigated minimum atomic concentration necessary to destabilize terminal solid solution phases. Later, Miracle and Senkov developed the topological criterion for glass formation [13]. Third principle (large negative mixing

enthalpy) is responsible for the formation of eutectics and dense packing of atoms of different kind. The importance of an efficient atomic packing for the formation of metallic glasses was shown recently [14, 15]. One should note that even, pure metals, for example, Ni, Fe can be made amorphous at high enough cooling rate estimated at 10^8–10^9 K/s [16–18] which are, however, not stable at room temperature unless separated into the nanometer scale spheres [19].

Egami created a theory of atomic level stresses in solid solutions and the stress criteria for the instability of the solid solution [20]. However, local distortions may exist even in crystalline pure metals and are quite common in intermetallics. For example, complex cI58 α-Mn is a good example of the structure which gives different nearest neighbor distance (atomic size) ranged from 224 to 282 pm between atoms of the same sort [21, 22].

Bulk glassy alloys with exceptionally high GFA, in general, are formed at the compositions with high reduced glass transition temperature $T_{rg} = T_g/T_l$ (T_g glass-transition temperature and T_l liquidus temperature) ratio exceeding approximately 0.6 [23]. The width of the supercooled liquid region (ΔT_x) (defined as $T_x - T_g$ where T_x is the onset devitrification/crystallization temperature) as indicator of the stability of the supercooled liquid against crystallization also correlates quite well with the observed GFA [4]. The parameter $\gamma = T_x/(T_g + T_l)$ [24] and various of its derivatives (see, for example [25, 26]) developed later take into account both T_{rg} and ΔT_x criteria.

One should also mention a topological criterion λ [11], the thermal conductivity of a molten alloy λ_l [27], electronegativity difference between the constituent elements ΔEN [10], criterion [28], and many other parameters [29] which have been summarized in Ref. [30] and separated for intrinsic and extrinsic factors. For example, the addition of Zr or Sc substituting for *Y* reduces the effective ΔEN values among the constituent elements and increases ΔT_x of an Al–Y–Ni–Co alloy [31]. However, a comparative study of the GFAs of the binary Si–Ni and Ge–Ni as well as ternary Si–Ni–Nd and Ge–Ni–Nd alloys showed that the principles for achieving high GFA known so far are rather necessary conditions which in some cases, however, are not sufficient [32].

Geometrical aspects of the atomic packing have been considered in binary metallic glasses, and it was found that they have solute to solvent radius ratios ranging from 0.602 to 1.456, produce structure-forming, solute-centered clusters with coordination numbers varying from 7 to 20, and a strong preference was found for special radius ratios, that give efficient local atomic packing in the first coordination shell [33].

Nevertheless, notwithstanding on significant progress achieved, there is still no clear understanding why some combinations of chemical elements are better glass-formers than others with similar molar fractions. In the present work, we test and discuss various binary alloys in which the glassy phase was not formed even by melt spinning technique with high cooling rate of the melt up to 1 MK/s, though by commonly accepted guidelines, these alloys could be as good glass-formers as other binary glasses.

Experimental procedure

The eutectic and nearly eutectic alloys (except for $Ag_{50}Y_{50}$), namely: $Ag_{88.5}Y_{11.5}$, $Ag_{71}Y_{29}$, $Ag_{65}Y_{35}$, $Ag_{50}Y_{50}$, $Ag_{27.5}Y_{72.5}$, $Cu_{56}Y_{44}$, $Si_{57}Mg_{43}$, $Si_{88}Sm_{12}$, $Si_{52}Pd_{48}$, $Si_{83}Nd_{17}$, $Si_{82}Y_{18}$, $Ge_{84}La_{16}$, $Ge_{64}Mg_{36}$, $Ge_{84}Nd_{16}$, $Ge_{83}Ce_{17}$, $Ge_{88}Y_{12}$, $Ge_{85}Pr_{15}$, and $Ge_{85}Sm_{15}$ were produced by arc-melting of pure metals and metalloids (99.9 wt% purity) in an argon atmosphere purified with Ti getter. In some cases, slightly off-eutectic (namely hypereutectic) alloys were chosen as glass formation is enhanced in slightly off-eutectic compositions. From these ingots, ribbon samples of about 20–30 μm thickness and 1 mm width were prepared by melt spinning on to a single copper roller at a roller tangential velocity of about 40 m/s. The structure of the ribbons was examined by X-ray diffractometry with monochromatic CuK_α radiation.

Results

None of the studied alloys was found to be fully glassy after rapid solidification by the melt spinning technique, though it enables a very high cooling rate of the order of 1 MK/s. Moreover, even the number of alloys which formed a partially amorphous structure was very limited. Figure 1 shows the XRD patterns of rapidly solidified Ag–Y alloys, for example. The crystalline phases formed in this group of alloys correspond to the equilibrium phase diagram except for the $Ag_{50}Y_{50}$ alloy which may be connected with a slight deviation from the stoichiometry. Only $Ag_{27.5}Y_{72.5}$ alloy formed a partially amorphous structure.

Volume effects in glass-transition have been considered before [34]. It has been argued that negative mixing volume is essential for glass formation as such an alloy will have a higher viscosity and a lower diffusivity [35]. Let us consider molar volume (MV) of the crystalline phases. These values are calculated for the intermetallic compounds in three known binary bulk glass-forming systems (Cu–Hf is similar to Cu–Zr), and the largest values were found to be −2.3 %(Cu_8Zr_3) [36], −3.5 % (Ni_3Nb) [37], and −17 % (Al_2Ca) [38] for Cu–Zr, Ni–Nb and Ca–Al systems, respectively. The difference in Molar Volume |ΔMV| values plot for Zr–Cu system (Fig. 2) is built by

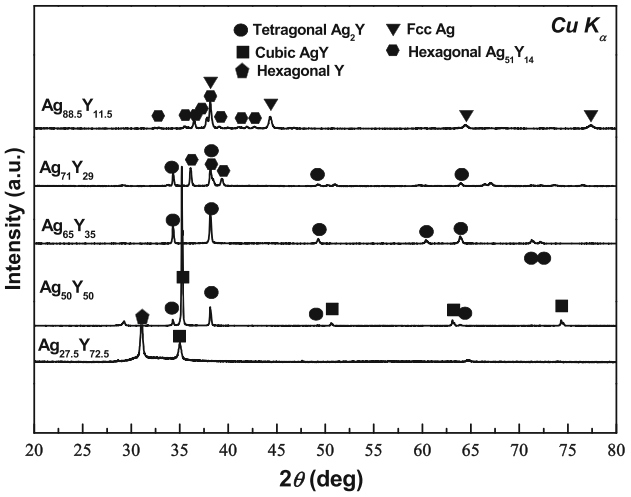

Fig. 1 XRD patterns of rapidly solidified Ag–Y alloys

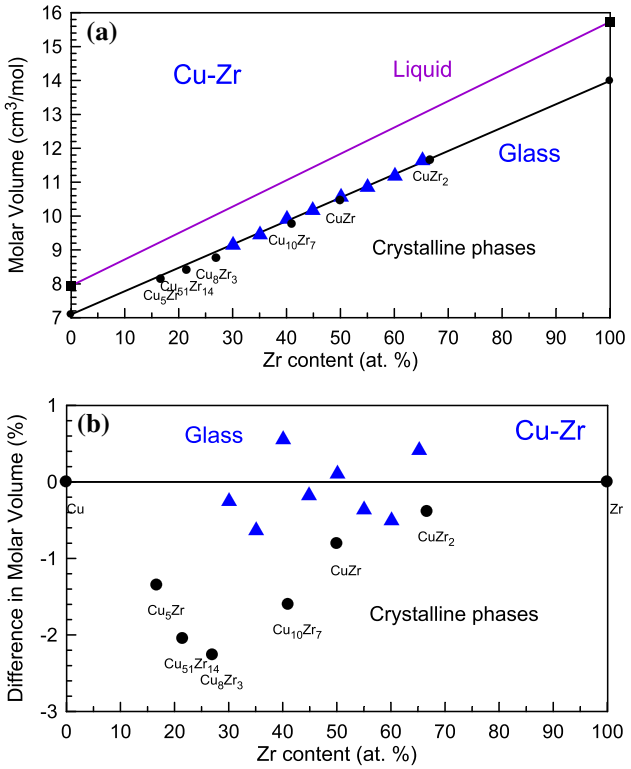

Fig. 2 Molar volume of the liquid, glassy, and crystalline phases in Cu–Zr system (**a**) and difference between that of crystals and the "ideal" solution (**b**)

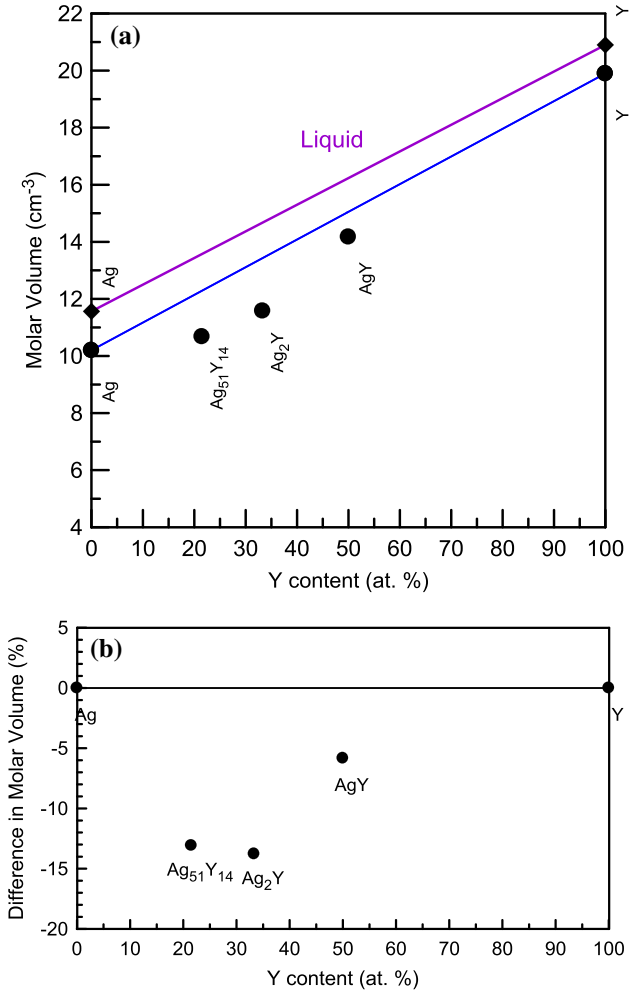

Fig. 3 Molar volume of the liquid, glassy, and crystalline phases in Ag–Y system (**a**) and difference between that of crystals and an ideal solution (**b**)

using the data for intermetallics [36, 39, 40] and glassy alloys [41].

Ag–Y system has several eutectics, negative mixing enthalpy among the constituent elements, forms densely packed intermetallic compounds (Fig. 3, the data from Refs. [42–44]), and nearly statistically ideal atomic size ratio close to 0.8 or 1.25 depending on the solvent element, while no single metallic glassy phase was formed. On the other hand, Ca–Al system with much larger atomic size difference readily forms a small size bulk metallic glass.

Crystalline phases in Cu–Y system also demonstrate large and negative difference in Molar Volume [45–47] but the glass formation is difficult in this system—only partially amorphous samples were obtained even by melt spinning. Metalloid-based Si,Ge–Mg, Si–Pd, and Si,Ge–RE alloys (RE-rare earth metal) also did not show single glassy phase formation.

Figure 4 shows the number of metallic glassy alloys as a function of the atomic size ratio. The data are taken from the database for 685 binary alloys [33]. One can mention at least three clear maxima at 0.7, 0.8, and 1.25. Similar data were obtained before with a smaller database [48, 49]. Looking at this diagram, one can see a small number of

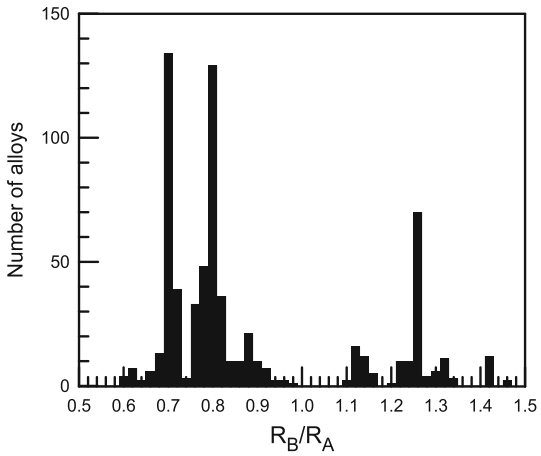

Fig. 4 Number of metallic glassy alloys produced by melt spinning as a function of atomic size ratio of solute to solvent atom (R_B/R_A). The integration distance was 0.02 nm

alloys with atomic size ratios from 0.9 to 1.1 and absence of alloys having R_B/R_A exceeding 1.45. Also, surprisingly low atomic size ratio of 1.14 [13] is found for Ni–Nb system in which a bulk glass-former (D_c = 1–2 mm) was found [50].

Several parameters for the alloy systems studied in the present work are summarized in Table 1 together with the results for the systems with good glass-formers studied previously from Ref. [33]. As one can see there is poor correlation between any parameter and the order of magnitude of critical thickness of the metallic glass.

In order to identify promising compositions with high glass-forming ability, the following structural and chemical factors [51, 52], such as the difference in atomic size (δ), the enthalpy of mixing (ΔH_{mix}), the entropy of mixing (ΔS_{mix}), and the difference in electronegativity of elements ($\Delta\chi$) are calculated. The values of these factors are determined by the following formulas:

$$\delta = \sqrt{\sum_{i=1}^{n} c_i \left(1 - \frac{r_i}{\bar{r}}\right)^2} \quad (1)$$

where c_i is the atomic fraction of the i-th component;
r_i is the atomic radius of the i-th component nm;
$\bar{r}$ is the mean radius of the atoms in the alloy nm.

$$\bar{r} = \sum_{i=1}^{n} c_i r_i \quad (2)$$

$$\Delta H_{mix} = \sum_{i=1, i\neq j}^{n} 4\Delta_{mix}^{AB} c_i c_j \quad (3)$$

where Δ_{mix}^{AB} is enthalpy of mixing of the alloy A-B,

$$\Delta S_{mix} = -R \sum_{i=1}^{n} c_i \ln c_i \quad (4)$$

where R is the gas constant, R = 8314 J/(mol K).

$$\Delta\chi = \sqrt{\sum_{i=1}^{n} c_i (\chi_i - \bar{\chi})^2}, \quad (5)$$

Table 1 Solute to solvent atom atomic size ratios (R_B/R_A), mixing enthalpy in liquid state (ΔH_{mix}^{L}), difference in molar volume between the weighted average and the most dense intermetallic compound ($|\Delta MV_{max}|$), difference in electronegativity ($|\Delta EN|$), critical thickness of the fully glassy sample (D_c), and the resulted type of the binary system alloys

System alloy	R_B/R_A	ΔH_{mix}^{L}, kJ/mol	AB compound	$\lvert\Delta MV_{max}\rvert$, %	$\lvert\Delta EN\rvert$	~D_c, m	Type
Ca–Al	0.701	−20	–	17	0.61	10^{-3}	BMG
Zr–Cu	0.797	−23	$cP2_{CM}^{HT}$	2.3	0.67	10^{-3}	BMG
Ti–Cu	0.887	−9	tP4	5.9	0.46	10^{-6}	RSG[a]
Zr–Ni	0.797	−49	$oC8_{CM}$	6.5	0.58	10^{-6}	RSG
Al–Y	1.270	−38	N/A[b]	5.9	0.39	10^{-6}	RSG
Y–Cu	0.704	−22	$cP2_{CM}$	6.3	0.78	?	–
Y–Ag	0.8	−29	$cP2_{CM}$	13.8	0.71	?	–
Ni–Nb	1.135	−30	–	3.5	0.31	10^{-3}	BMG
Si–Y	1.565	−73	$oC8_{CM}$	18.2	0.68	?	–
Ge–Y	1.452	−73	$oC8_{IM}$	12	0.79	?	–
Pd–Si	0.775	−55	N/A	16	0.30	10^{-3}	BMG
Si–Pd	1.290	−55	$oP8_{IM}^{HT}$	16	0.30	?	–
Au–Al	0.993	−22	$mP8_{IM}$	2.5	0.93	?	–

RSG denotes rapidly solidified metallic glass, while AB denotes the type of the equiatomic compound. HT denotes high temperature, while CM and IM indicate congruently melting and incongruently melting compound, respectively. In many cases, congruent or incongruent melting is only assumed in the phase diagrams but not verified

[a] Rapidly solidified glass (melt spun ribbons)

[b] Not applicable, because the glasses are formed near Al- or Pd-rich size of the phase diagram far from AB compound

where χ_i is Pauling electronegativity of the i-th component; $\bar{\chi}$ is the average electronegativity of the components in the alloy.

$$\bar{\chi} = \sum_{i=1}^{n} c_i \chi_i. \quad (6)$$

The r_i, Δ^{AB}_{mix}, and χ_i values were taken from Refs [53, 54]. The calculation results are given in Table 2 together with critical thickness of the glassy samples [33].

The plots of the critical thickness as a function of the ΔH_{mix} and ΔS_{mix} given in Table 2 are shown in Fig. 5. No clear correlation is found between the D_c and the parameters. One may only notice that too large value of ΔH_{mix} is harmful for glass formation. Also, binary BMG alloys tend to have ΔS_{mix} close to 4 and 5.5.

Discussion

Ag and Y have a large difference in the electronegativity of 1.93 and 1.22 (Pauling scale), respectively [55], negative mixing enthalpy in the liquid state of −29 kJ/mol (for equiatomic composition), nearly ideal atomic size ratio R of 0.8 or 1.25 (depending on the base element) required for achieving good GFA, form a number of intermetallic compounds, and several eutectic compositions without high melting temperature intermetallic compounds (not exceeding the weighted average melting temperature of Ag and Y of the same composition) [42–44, 56, 57]. $\Delta T = T_{wa} - T_e$ (T_{wa} and T_e are weighted average liquidus and eutectic temperature, respectively) is as large as about 450 K and $\Delta T_r = (T_{wa} - T_e)/T_{wa}$ is close to 0.3. The molar volume difference between the ideal solid solution and the intermetallic compounds in Ag–Y system is much higher than that in Cu–Zr but close to that in Al–Ca one and yet no single glassy phase is formed, while even bulk metallic glasses can be formed in Cu–Zr and Al–Ca systems [33]. Molar volume of Cu–Zr metallic glasses is close to that of the ideal solid solution for crystalline metals, and the density of intermetallic compounds in this system is not as large as in Al–Ca alloys yet BMG samples can be formed. On the other hand, Al-rich Al–Y alloys having nearly the same atomic size ratio do form metallic glasses on rapid solidification notwithstanding on the existence of the Al_2Y intermetallic compound with high melting temperature of 1758 K.

These results are similar to those obtained for Cu–Y alloys, except for $Cu_{33}Y_{67}$ [58]. Liquid Cu–Y system alloys also have a negative mixing enthalpy of −22 kJ/mol (for equiatomic binary alloy) which is close to that of liquid alloy in Cu–Zr system but the GFA of the eutectic Cu–Y alloys is much lower. Moreover, eutectic temperatures are quite close in the phase diagrams of both systems, and equiatomic cP2 cubic phase is formed in both systems, while it is more stable in Cu–Y one [56]. The corresponding lattice parameters are 0.3477 nm for CuY [45] and 0.3262 nm for CuZr [59] phase. However, no BMG phase was found in Cu–Y alloys notwithstanding on large negative mixing enthalpy and large atomic size ratio of 0.704 or 1.421. The results are also similar for the metalloid-rich alloys. Si and Ge also form quite dense compounds with Y and well as with Pd (Table 1).

Table 1 also indicates that the formation of densely packed intermetallic compounds with complex structure in the alloy systems neither favor nor disfavor glass formation. More loosely packed systems readily form metallic glasses at right atomic size ratio. For example, all the AgY, CuY, and CuZr compounds have a cP2 structure (simple cubic lattice, ordered BCC) which is easy to nucleate from the melt owing to its small unit cell consisting of 2 atoms and simple cubic structure. However, the CuZr phase is less stable in comparison with the former two compounds as it decomposes by the eutectoid reaction at low temperature. According to Table 1, BMG alloys are formed in the systems where no such compound exists. At the same time, cP2 phase is not formed in the most of Ag–Y alloys on rapid solidification (Fig. 1) which indicates that this is not the competing crystalline compound in most of these alloys. The binary eutectic temperatures at the compositional center of the Cu–Zr and Ag–Y phase diagrams are close to each other but about 10–20 K lower in case of Cu–Zr alloys [60].

Binary bulk metallic glass (BMG) alloys were formed in the following systems: Ca–Al, Cu–Hf, Cu–Zr, Hf–Cu, Ni–Nb, Pd–Si, and Zr–Cu with atomic size difference R_B/R_A of 0.701, 1.254, 1.254, 0.797, 1.135, 0.775, and 0.797. One can see various atomic size ratios close to 25 % difference, while Ni–Nb atomic pair has clearly too small one. Binary glasses were found to be most commonly produced with radius ratios near $R \cong 0.799$ that give structures with coordination number of 10 [33]. In such a case, the efficiently packed clusters consisting of a central solute atom surrounded by ~10 solvent atoms are formed. This is the case for Y–Ag alloys, which, however, did not form metallic glasses even by rapid solidification (except for partial glassy phase in the Y-rich alloy).

Other commonly observed structures include the glasses with coordination numbers of 9, 12, 15, and 17 with radius ratios near R_B/R_A 0.710, 0.902, 1.116, and 1.248, respectively. The most stable glasses represent 4 values of R, including 0.710 for CN = 9 structures; 0.799 for CN = 10 structures; 1.116 for CN = 15 structures; and 1.248 for CN = 17 structures [33, 61]. Again various binary system alloys produced in the present work are not glassy.

The influence of efficient atomic packing on the constitution of metallic glasses was studied, and it was found

Table 2 The structural and chemical factors, such as the difference in atomic size (δ), the enthalpy of mixing ΔH_{mix}, the entropy of mixing (ΔS_{mix}), the difference in electronegativity of elements ($\Delta\chi$), and critical thickness D_c for glass formation for different alloys

	Alloy	ΔH_{mix} (kJ/Mol)	ΔS_{mix} J/(Mol·K)	$\Delta\chi$	δ	D_c (mm)
Low GFA	$Ag_{88.5}Y_{11.5}$	−11.81	2.97	0.23	7.66	<0.02
	$Ag_{71}Y_{29}$	−23.88	5.01	0.32	10.46	<0.02
	$Ag_{65}Y_{35}$	−26.39	5.38	0.34	10.85	<0.02
	$Ag_{50}Y_{50}$	−29.00	5.76	0.36	11.00	<0.02
	$Ag_{27.5}Y_{72.5}$	−23.13	4.89	0.32	9.36	<0.02
	$Y_{44}Cu_{56}$	−21.68	5.70	0.34	17.24	<0.02
	$Si_{57}Mg_{43}$	−25.49	5.68	0.29	16.48	<0.02
	$Si_{88}Sm_{12}$	−41.77	3.05	0.24	17.33	<0.02
	$Si_{52}Pd_{48}$	−54.91	5.76	0.15	8.81	<0.02
	$Si_{83}Nd_{17}$	−41.20	3.79	0.29	14.80	<0.02
	$Y_{18}Si_{82}$	−43.10	3.92	0.26	19.64	<0.02
	$Ge_{84}La_{16}$	−39.51	3.66	0.33	17.45	<0.02
	$Mg_{36}Ge_{64}$	−24.42	5.43	0.34	12.65	<0.02
	$Nd_{16}Ge_{84}$	−54.57	3.66	0.32	11.25	<0.02
	$Ge_{83}Ce_{17}$	−41.48	3.79	0.33	16.41	<0.02
	$Y_{12}Ge_{88}$	−30.62	3.05	0.26	13.97	<0.02
	$Ge_{85}Pr_{15}$	−36.98	3.51	0.31	11.25	<0.02
	$Sm_{15}Ge_{85}$	−36.98	3.51	0.30	15.36	<0.02
Binary BMGs	$Ca_{66.4}Al_{33.6}$	−17.85	5.31	0.29	14.33	1
	$Cu_{65}Hf_{35}$	−15.47	5.38	0.29	10.35	2
	$Cu_{60}Hf_{40}$	−16.32	5.60	0.29	10.51	1
	$Cu_{64.5}Zr_{35.5}$	−21.07	5.41	0.27	11.16	2
	$Cu_{64}Zr_{36}$	−21.1968	5.43	0.27	11.18	1.6
	$Cu_{60}Zr_{40}$	−22.08	5.60	0.28	11.31	1
	$Cu_{55}Hf_{45}$	−16.83	5.72	0.30	10.56	1.5
	$Ni_{62}Nb_{38}$	−28.27	5.52	0.15	6.75	2
	$Ni_{60}Nb_{40}$	−27.84	5.60	0.15	6.80	1
	$Si_{18}Pd_{82}$	−32.47	3.92	0.12	6.39	7^F
	$Si_{19}Pd_{81}$	−33.86	4.04	0.12	6.53	8^F
	$Si_{20}Pd_{80}$	−35.20	4.16	0.12	6.67	8^F
	$Cu_{45}Zr_{55}$	−22.77	5.72	0.28	11.10	1.5
	$Cu_{46}Zr_{54}$	−22.85	5.74	0.28	11.14	2
	$Cu_{50}Zr_{50}$	−23.00	5.76	0.29	11.28	1.2
	$Cu_{56}Zr_{44}$	−22.67	5.70	0.28	11.35	1

Symbol ^{F} denotes that fluxing treatment is required for achieving high GFA

that a high atom packing efficiency is a fundamental principle in the formation of metallic glasses [48]. Efficient atomic packing produces a smaller system volume, reducing the volume energy associated with an atomic ensemble and providing a physical basis for this concept. From a kinetic perspective, efficiently packed atoms are expected to produce a highly viscous melt. The values of $R = 0.884$ ($N = 11$) and $R = 1.116$ ($N = 15$) accurately represent bounds of $\sim$12 %. This concept is based on atom packing efficiency in the first coordination shell of solute-centered clusters. However, the efficient packing of clusters and filling of the space between clusters are also important as otherwise there could be voids between efficiently packed in the first coordination shell.

However, the concept of atomic size has some clear deficiencies. (1) There is meaningless to talk about size of a single atom. One can discuss only half of the nearest interatomic distances in the lattice of similar kinds of atoms or atomic sizes of atoms of different kinds in a compound. This approach has been utilized by Goldschmidt [62]. (2) As we are talking about metallic glasses, all bounds are considered to be non-directional. Nevertheless, existence of some degree of covalent or even partly ionic bonding in the intermetallic compounds (and thus in metallic glasses) has been discussed for years [63, 64]. (3) Only atoms with outer shells of s-type can be considered spherical, while elements having, for example, p-type outer shell are not spherical by default which makes

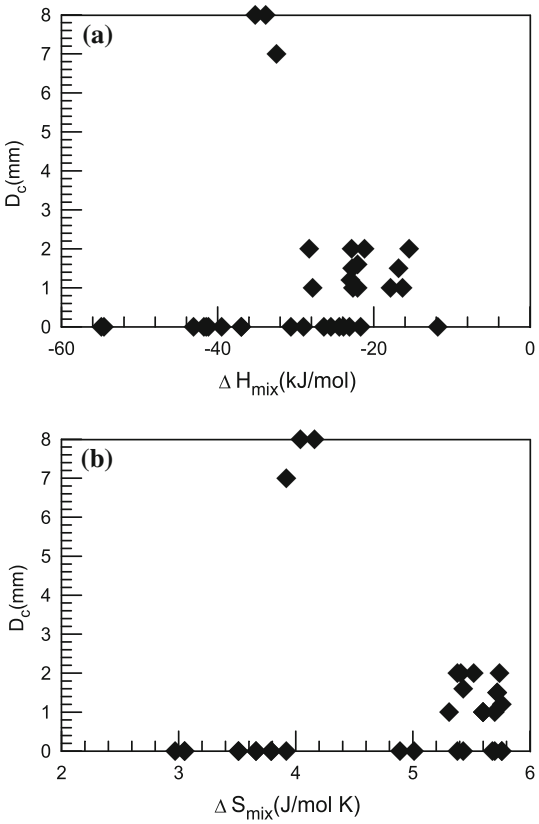

Fig. 5 Critical thickness for glass formation in various alloys as a function of ΔH_{mix} and ΔS_{mix}. For the alloys with low glass-forming ability, 0 is used as D_c

determination of their atomic sizes more complicated. (4) Atomic size of an element derived from the bond length with different elements varies owing to different bond character, charge transfer, etc.. Significant bond shortening has been observed in case of Al–Fe–Ce [65] and Au–Al alloys [66].

Too large mixing enthalpy may be the reason for the chemical short-range order observed in the Ni–Zr alloys resulting from the hybridization of 3d band of nickel with the 4d band of zirconium [67] leading to lower GFA of these alloys compared to Cu–Zr. The formation of partly covalent bonds leading to large mixing enthalpy may be responsible for lower GFA of the Si- and Ge-rich glasses. On the other hand, the structural changes and vitrification of the Pd–Cu–Ni–P liquid alloy on cooling from above the equilibrium liquidus temperature studied in situ by synchrotron radiation X-ray diffraction, and the results of ab initio computer simulation clearly indicated intensification of covalent bonding close to glass-transition which is responsible for large fragility of the melt [68]. It allows us to anticipate that the Si- and Ge-rich glasses can also be fragile which deteriorates their GFA. This factor explains the low GFA of alloys even having high enough T_g [17].

No glass formation was found in rapidly solidified $Au_{75}Al_{25}$ and $Au_{57}Al_{43}$ alloys [66], though Au–Ti alloys having nearly the same atomic size ratio close to 1 have been vitrified upon laser beam melting [69]. Although in general, compositions of metallic glasses follow deep eutectics [70], Au–Al system alloys located in compositions close to deep eutectics but having similar atomic size do not produce a glassy phase. The liquidus temperature of some Au–Al system alloys is as low as about 525 °C (798 K), which is significantly lower than those for the pure elements. It indicates that this thermodynamically stable liquid is significantly under-cooled compared to that of pure elements and yet its Gibbs Free Energy is still lower than that of any of the competing crystalline phases. One viewpoint could be connected with the theory that glass formation is favored in systems where the formation of complex compounds with large unit cells takes place, while atoms with similar atomic size trigger formation of simple crystalline compounds which formation in its turn successfully competes with the glass formation.

No glassy phase was produced in Si,Ge–RE or Si,Ge–Mg alloys studied though they satisfy general requirements for glass formation i.e., form relatively "deep" eutectics, have large mixing enthalpy [71] and large atomic size difference which should favor glass formation. However, these alloys represent an extreme case of large difference in the atomic size. For example, solute to solvent atomic size ratios for Si–Y and Ge–Y alloys are 1.56 and 1.45 [72, 73], respectively. It has been suggested that atomic radius of metallic Ge can be 143 pm [74] or 139 pm [73], while 124 pm is a more reasonable value in metallic glasses from the viewpoint of experimental observations of Ge–Cr and Ge–Al distances [75] which is close to that of tetrahedral Ge. This may indicate significant charge transfer in Ge- and Si-bearing alloys.

Moreover, $Si_{52}Pd_{48}$ alloy is supposed to have a good GFA according to the topological instability criterion combined with the average electronegativity difference of an element and its surrounding neighbors [76] which is, however, not supported by the present data. If one calculates minimum concentration C_{min} for amorphization using a correlation between the glass formability and the extent of atomic size mismatch of the constituent atoms in Si–Y system ($C_{min} = 0.1/((R_B/R_A)^3 - 1)$ [11], it will be about 3.5 % and yet no glass formation is found. Although Si–Y and Ge–Y eutectics are quite close to the metalloid terminal part of the corresponding phase diagrams, Al–RE alloys with much smaller size difference of about 1.26 produce metallic glasses by melt spinning in Al-rich area [33].

Notwithstanding on the formation of a deep eutectic and low stability of oP8 PdSi compound, $Si_{52}Pd_{48}$ alloy ($C_{min} = 13.7$ % if $R_{Si} = 115$ pm) did not produce a glassy phase, though Pd–Si alloys are good glass-formers and even bulk glass-formers when fluxed [77, 78]. Earlier investigations showed metallic glass formation in multi-component metalloid-based alloys which are, however, still marginal glass-formers [79]. ΔT and ΔT_r parameters for Si–Pd system are quite large of about 590 K and 0.4, respectively. Also, although the number of intermetallic compounds in Pd-rich area of the Pd–Si system is much larger and the temperature stability interval of PdSi phase is narrow, the enthalpy of mixing is highly negative in both Pd- and Si-rich areas, and the shape of the ΔH_{mix} curve as a function of composition is nearly symmetrical with central mirror plane [80]. For comparison, there are only two equilibrium intermetallic compounds in Ca–Al system (Al_4Ca and Al_2Ca), and yet bulk metallic glass formation was possible in Ca-rich side where there are no equilibrium compounds [81].

On the other hand in the range of metallic glass formation, the terminal solid solution is not the phase which competes with the glassy phase. This role is played by intermetallic compounds, and for the formation of intermetallic compounds, the difference in atomic size is not an issue. As well as metallic glasses chemical compounds are also formed at significantly different atomic sizes of the elements or when the elements have a large difference in the electronegativity like Au and Al. Many of binary glass-forming systems have plenty of equilibrium intermetallic compounds even in case of Pd–P, Pd–Si, Fe–B and other similar systems with a large atomic size difference.

RE/Si atomic size ratios in Si–RE alloys range from 1.48 to 1.75. These values are out of the glass formation range in the diagrams in Fig. 4. On the other hand, smaller atomic size ratio 1.39 for Mg/Si, 1.37–1.45 for RE/Ge, and even 1.2 for Pd/Si also do not favor glass formation in the corresponding alloys though Si–RE and Ge–RE phase diagrams are quite similar in metal-rich and metalloid-rich area. These particular ratios are also not well represented in Fig. 4. These results support the idea of efficient packing and indicate that not only large but also certain atomic size ratios favor glass formation.

Glass formation is hampered in metalloid-rich areas likely owing to unfavorable atomic size ratios as, in general, metallic glasses are more readily formed in alloys having solute to solvent size ratio below unity than above. The number of glassy alloys with $R_B/R_A < 1$ is three times larger than with $R_B/R_A > 1$ (Fig. 4).

One can also see that owing to the rules of the Periodic Table [82], the atomic radius and electronegativity [55, 83] of chemical elements are somewhat interrelated (Fig. 6). The plot has been fitted with an exponential function. After linearization, the coefficient of determination is 0.72. Thus, atomic size difference and mixing enthalpy are also mutually correlated factors.

As it is shown there is no common group of the factors which could explain the difference in the GFA among the studied alloys and the BMG formers reported earlier. The existence of the unaccounted factors influencing the GFA of alloys had been suspected long ago. One of them should be related to the electronic structure [84, 85]. This idea can be supported by the following observations. For example, the addition of 1 at% of Cu or Pd to Al–Y–Ni–Co alloy [86, 87] or Cu to Al–Y–Fe alloys [88, 89] drastically reduces their GFA and causes precipitation of the primary α-Al particles, while none of the other parameters such as

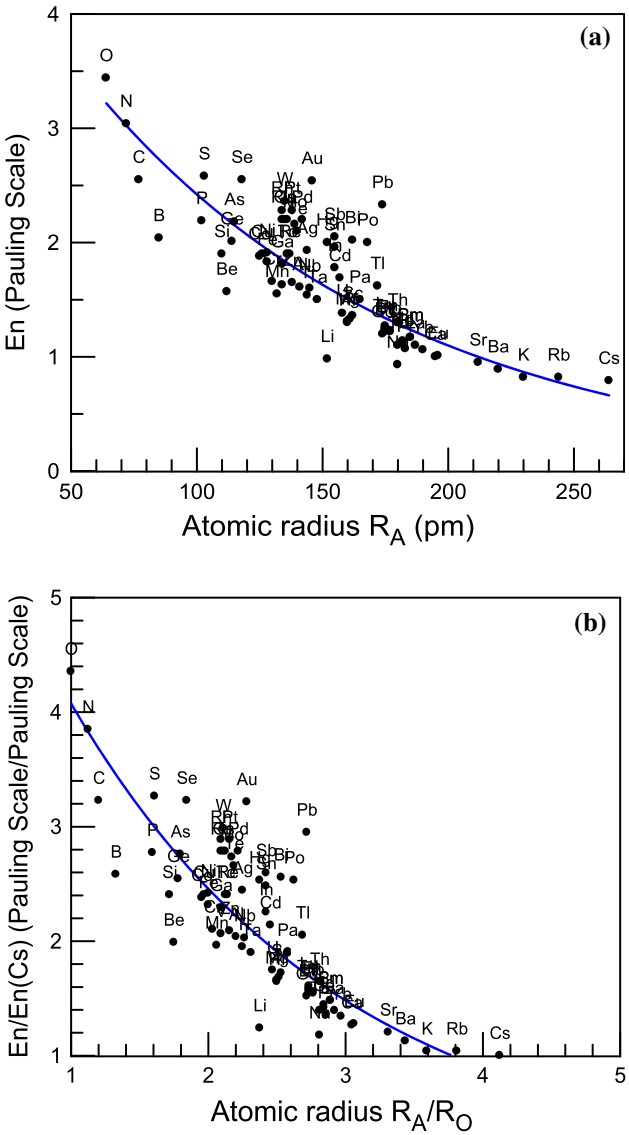

Fig. 6 Pauling electronegativity En as a function of atomic radius of the element in absolute (**a**) and relative (**b**) values. The data are taken from Ref. [55, 33]

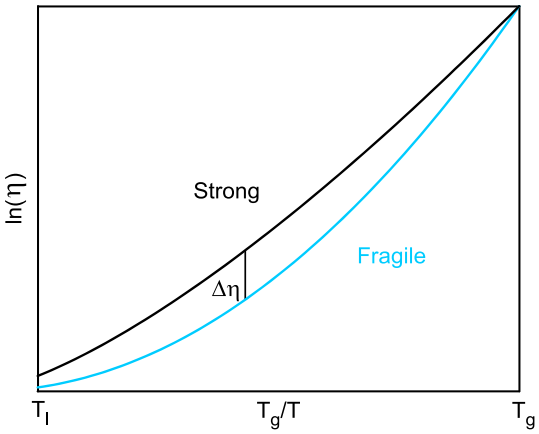

Fig. 7 Schematic plot indicating an inverse temperature dependence of melt viscosity (η) as a function of temperature

average atomic size or overall mixing enthalpy are affected. Replacing Ni in the $Al_{85}Ni_9La_6$ alloy with Cu also decreases its thermal stability [90]. Small amount of Si affects crystallization of $Al_{86}Ni_2Co_{5.8}Gd_{5.7}$ alloy [91]. Al forms readily intermetallic compounds with Cu as well as with Fe, Ni, or Y, and the effect cannot be connected with possible repulsive atomic interactions. Charge transfer between the metals with significantly different electronegativity may lead to the changes in the atomic size [66]. If one considers the electronegativity difference, which is higher in case of Ag–Y alloys compared to Cu–Zr, Y may form a more strongly covalent bond with Ag and, owing to change transfer, become considerably larger—making the radius ratios inappropriate for glass formation. For example, the high thermal stability of Zr–Pt compounds is attributed to a combination of localized, highly polar, sd–sd bonds between Zr and Pt that enhance the normal metallic (sp–sp) bonding [92].

Also, intensification of a covalent bonding between metallic atoms and P was found in Pd–Cu–Ni–P melts cooled in situ close to the glass-transition region [68, 93] which was responsible for the changes in the structure of a liquid (clustering, [94]), and thus, fragile behavior of this melt. Fragile liquids are generally predisposed to have lower GFA compared to strong liquids [95]. It can be easily illustrated by using a schematic Angel plot shown in Fig. 7. Even at the same values of T_{rg}, fragile liquid is going to have lower viscosity on cooling in the entire range between T_l and T_g. In general, low viscosity of the melt facilitates both nucleation and growth rate of crystals [96].

Conclusions

Most of the alloys studied in the present work have a large difference in the electronegativity between the constituent elements, large negative mixing enthalpy in the liquid state, large atomic size difference, or nearly ideal atomic size ratio (such as, for example, R of 0.8 or 1.25 depending on the base element in Ag–Y system) required for achieving good GFA, form a number of intermetallic compounds with relatively low melting temperature and several eutectic compositions, but yet do not form metallic glasses even by rapid solidification.

Formation of densely packed intermetallic compounds with complex structure in the alloy systems neither favors nor disfavors glass formation. Systems with more loosely packed crystalline phases, like Zr–Cu, readily form metallic glasses if right atomic size ratio is attained at right composition.

Glass formation is hampered in metalloid-rich alloys likely owing to unfavorably large or small atomic size ratios strongly deviating from the unity and possible covalent bonding leading to large fragility of the melt. The atomic size ratios close to 1 like in Au–Al system also disfavor glass formation.

No clear correlation with critical thickness for glass formation was found for the difference in the atomic size, the entropy of mixing, and the difference in electronegativity of the elements. One can note, however, that too large value of ΔH_{mix} is rather harmful for glass formation, while binary BMG alloys tend to have ΔS_{mix} close to 4 and 5.5. Electronic structure of the melt, structural changes on cooling related to the fragility of the melt might be responsible for the observed glass-forming ability.

Acknowledgements This work was supported by the World Premier International Research Center Initiative (WPI), MEXT, Japan and by the Ministry of Education and Science of the Russian Federation in the framework of Increase Competitiveness Program of NUST « MISiS » (№ К2-2014-013). The authors sincerely thank Daniel Miracle and Kevin Laws for their critical comments.

References

1. Inoue A (1995) High-strength bulk amorphous alloys with low critical cooling rates. Mater Trans JIM 36:866–875
2. Greer AL (1995) Metallic glasses. Science 267:1947–1953
3. Inoue A (2000) Stabilization of metallic supercooled liquid and bulk amorphous alloys. Acta Mater 48:279–306
4. Johnson WL (1999) Bulk glass-forming metallic alloys: science and technology. MRS Bull 24:42–56
5. Louzguine-Luzgin DV, Inoue A (2013) Bulk metallic glasses. formation, structure, properties, and applications. In: Buschow KHJ (ed) Handbook of magnetic materials. Elsevier, New York, pp 131–171
6. Louzguine-Luzgin DV, Louzguina-Luzgina LV, Ketov SV, Zadorozhnyy VYu, Greer AL (2014) Influence of cyclic loading on the onset of failure in a Zr-based bulk metallic glass. J Mater Sci 49:6716–6721. doi:10.1007/s10853-014-8276-2
7. Louzguine-Luzgin DV, Xie G, Zhang Q, Suryanarayana C, Inoue A (2010) Formation, structure, and crystallization behavior of

Cu-based bulk glass-forming alloys. Metall Mater Trans A 41:1664–1669
8. Louzguine-Luzgin DV, Miracle DB, Louzguina-Luzgina L, Inoue A (2010) Comparative analysis of glass-formation in binary, ternary, and multicomponent alloys. J Appl Phys 108:103511
9. Louzguine DV, Inoue A (2002) Comparison of the long-term thermal stability of various metallic glasses under continuous heating. Scripta Mater 47:887–891
10. Louzguine DV, Inoue A (2001) Electronegativity of the constituent rare-earth metals as a factor stabilizing the supercooled liquid region in Al-based metallic glasses. Appl Phys Lett 79:3410–3412
11. Egami T, Waseda Y (1984) Atomic size effect on the formability of metallic glasses. J Non-Cryst Solids 64:113–134
12. Egami T (1996) The atomic structure of aluminum based metallic glasses and universal criterion for glass-formation. J Non-Cryst Solids 205–207:575–582
13. Miracle DB, Senkov ON (2003) Topological criterion for metallic glass formation. Mater Sci Eng A 347:50–58
14. Miracle DB (2006) The efficient cluster packing model. An atomic structural model for metallic glasses. Acta Mater 54:4317–4336
15. Sheng HW, Luo WK, Alamgir FM, Bai JM, Ma E (2006) Atomic packing and short-to- medium-range order in metallic glasses. Nature 439:419–425
16. Tamura K, Endo H (1969) Ferromagnetic Properties of Amorphous Nickel. Phys Lett A 29:52–53
17. Davies HA (1983) Metallic glass formation. In: Luborsky FE (ed) Amorphous metallic alloys. Butterworths, London, pp 8–25
18. Louzguine-Luzgin DV, Belosludov R, Saito M, Kawazoe Y, Inoue A (2008) Glass-transition behavior of Ni: Calculation, prediction, and experiment. J Appl Phys 104:123529–1–123529-5
19. Kim YW, Lin HM, Kelly TF (1989) Amorphous solidification of pure metals in submicron spheres. Acta Metall 37:247–255
20. Egami T (1997) Universal criterion for metallic glass formation. Mater Sci Eng, A 226–228:261–267
21. Hobbs D, Hafner J, Spisak D (2003) Understanding the complex metallic element Mn. I. Crystalline and noncollinear magnetic structure of α-Mn. Phys Rev B 68:014407
22. Louzguine-Luzgin DV, Yavari AR, Vaughan G, Inoue A (2009) Clustered crystalline structures as glassy phase approximants. Intermetallics 17:477–480
23. Turnbull D, Cohen MH (1961) Free-volume model of the amorphous phase: glass transition. J Chem Phys 34:120–125
24. Lu ZP, Liu CT (2002) A new glass-forming ability criterion for bulk metallic glasses. Acta Mater 50:3501–3512
25. Suryanarayana C, Seki I, Inoue A (2009) A critical analysis of the glass-forming ability of alloys. J Non-Cryst Solids 355:355–360
26. Suryanarayana C, Inoue A (2010) Bulk Metallic Glasses. CRC Press, Boca Raton
27. Louzguine-Luzgin DV, Setyawan AD, Kato H, Inoue A (2007) Thermal conductivity of an alloy in relation to the observed cooling rate and glass-forming ability. Phil Mag 87:1845–1854
28. Park ES, Kim DH, Kim WT (2005) Parameter for glass forming ability of ternary alloy systems. Appl Phys Lett 86:061907
29. Senkov ON, Miracle DB, Mullens HM (2005) Topological criteria for amorphization based on a thermodynamic approach. J Appl Phys 97:103502
30. Louzguine-Luzgin DV, Miracle DB, Inoue A (2008) Intrinsic and Extrinsic Factors Influencing the Glass-Forming Ability of Alloys. Adv Eng Mater 10:1008–1015
31. Louzguine-Luzgin DV, Inoue A, Botta WJ (2006) Reduced electronegativity difference as a factor leading to the formation of Al-based glassy alloys with a large supercooled liquid region of 50 K. Appl Phys Lett 88:011911
32. Louzguine DV, Louzguina LV, Inoue A (2002) Factors influencing glass formation in rapidly solidified Si, Ge–Ni and Si, Ge–Ni–Nd alloys. Appl Phys Lett 80:1556–1558
33. Miracle DB, Louzguine-Luzgin DV, Louzguina-Luzgina LV, Inoue A (2010) An assessment of binary metallic glasses: correlations between structure, glass forming ability and stability. Int Mater Rev 55:218–256
34. Battezzati L, Baricco M (1988) An analysis of volume effects in metallic glass formation. J Less-Common Met 145:31–38
35. Yavari AR (1983) Small volume change on melting as a new criterion for easy formation of metallic glasses. Phys Lett A 95:165–168
36. Bsenko L (1976) The crystal structure of Hf_3Cu_8 and Zr_3Cu_8. Acta Cryst B 32:2220–2224
37. Fang T, Kennedy SJ, Quan L, Hicks TJ (1992) The structure and paramagnetism of Ni_3Nb. J Phys-Condens Matter 4:2405–2409
38. Zhou DW, Liu JS, Peng P, Chen L, Hu Y (2008) A first-principles study on the structural stability of Al_2Ca, Al_4Ca and Mg_2Ca phases. J Mater Lett 62:206–210
39. Glimois JL, Forey P, Feron J, Becle C (1981) Structural investigations of the pseudo-binary compounds $Ni_{10-x}Cu_xZr_7$. J Less-Common Met 78:45–50
40. Gabathuler JP, White P, Parthé E (1975) $Zr_{14}Cu_{51}$ and $Hf_{14}Cu_{51}$ with $GdAg_{3.6}$ structure type. Acta Cryst B 31:608–610
41. Mattern N, Schops A, Kuhn U, Acker J, Khvostikova O, Eckert J (2008) Structural behavior of Cu_xZr_{100-x} metallic glass ($x = 35 - 70$). J Non-Cryst Solids 354:1054–1060
42. Gebhardt E, von Erdberg M, Lüty U (1964) Silver-Yttrium binary alloy phase diagram (based on 1964 Gebhardt E.). IMD Spec Rep Ser 10:303–314
43. Steeb S, Godel D, Löhr C (1968) On the structure of the compounds Ag3R.E. (R.E. = Y, La, Ce, Sm, Gd, Dy, Ho, Er). J Less-Common Met 15:137
44. McMasters OD, Gschneidner KA Jr, Venteicher RF (1970) Crystallography of the silver-rich rare-earth-silver intermetallic compounds. Acta Crystall B 26:1224–1229
45. Kadomatsu H, Kawanishi Y, Kurisu M, Tokunaga T, Fujiwara H (1988) Structural phase transitions in $YCu_{1-x}M_x$ (M = Ni, Ag and Ga). J Less Common Met 141:29–36
46. Gratz E, Rotter M, Lindbaum A (1993) The influence of the crystal field on the anisotropic thermal expansion in $TmCu_2$. J Phys 5:7955–7958
47. Buschow KHJ, van der Goot AS (1971) Composition and crystal structure of hexagonal Cu-rich rare earth-copper compounds. Acta Cryst. B 27:1085–1088
48. Miracle DB, Sanders WS, Senkov ON (2003) The influence of efficient atomic packing on the Constitution of metallic glasses. Philos Mag 83:2409–2428
49. Miracle DB (2004) A structural model for metallic glasses. Nat Mater 3:697–702
50. Xia L, Li WH, Fang SS, Wei BC, Dong YD (2006) Binary Ni–Nb bulk metallic glasses. J Appl Phys 99:026103–026103-3
51. Zhang Y, Zhou YJ, Lin JP (2008) Solid solution phase formation rules for multicomponent alloys. Adv Eng Mater 10:534–538
52. Fang SS, Xiao X, Lei X (2003) Relationship between the widths of supercooled liquid regions and bond parameters of Mg-based bulk metallic glasses. J Non-Cryst Solids 321:120–125
53. Takeuchi A, Inoue A (2005) Classification of bulk metallic glasses by atomic size difference, heat of mixing and period of constituent elements and its application to characterization of the main alloying element. Mater Trans 46:2817–2829
54. Guo S, Liu CT (2011) Phase stability in high entropy alloys: Formation of solid-solution phase or amorphous phase. Mater Int 21:433–446
55. http://www.webelements.com/periodicity/electronegativity_pauling/
56. Gale WF, Totemeier TC (2004) (eds.), Smithells metals reference book. 8th edn. Elsevier Butterworth-Heinemann Ltd., Oxford, pp 11-28–11-29

57. Ketov SV, Louzguina-Luzgina LV, Churyumov AYu, Solonin AN, Miracle DB, Louzguine-Luzgin DV, Inoue A (2012) Glass-formation and crystallization processes in Ag-Y-Cu alloys. J Non-Cryst Solids 358:1759–1763
58. Satta M, Rizzi P, Baricco M (2009) Glass-formation and hardness of Cu–Y alloys. J Alloys Compd 483:50–53
59. Carvalho EM, Harris IR (1980) Constitutional and structural studies of the intermetallic phase ZrCu. J Mater Sci 15:1224–1230. doi:10.1007/BF00551811
60. Burlington MA (2004) Smithells metals reference book. In: Gale WF, Totemeier TC (eds) ASM international metals reference book, 8th edn. Elsevier Butterworth-Heinemann Ltd., Oxford, pp 11-271–11-272
61. Miracle DB, Lord EA, Ranganathan S (2006) Candidate atomic cluster configurations in metallic glass structures. Mater Trans 47:1737–1742
62. Goldschmidt V (1928) Uber atomabstande in metallen. Z Phys Chem 133:397–419
63. Pauling L (1947) Atomic radii and interatomic distances in metals. J Am Chem Soc 69:542–553
64. Eiblert R, Redinger J, Neckel A (1987) Electronic structure, chemical bonding and spectral properties of the intermetallic compounds FeTi CoTi and NiTi. J Phys F 17:1533
65. Egami T (1996) Universal criterion for metallic glass formation. J Non-Cryst Solids 205–207:575–582
66. Egami T, Ojha M, Nicholson DM, Louzguine-Luzgin DV, Chen N, Inoue A (2012) Glass formability and the Al-Au system. Philos Mag 92:655–665
67. Nurgayanov PP, Chudinov VG (2000) Atomic mechanisms of glass formation in metallic alloys, tendency to glass formation, and structural models. J Glass Phys Chem 26:335–341
68. Louzguine-Luzgin DV, Belosludov R, Yavari AR, Georgarakis K, Vaughan G, Kawazoe Y, Egami T, Inoue A (2011) Structural basis for supercooled liquid fragility established by synchrotron-radiation method and computer simulation. J Appl Phys 110:043519
69. Blatter A, von Allmen M (1985) Reversible amorphization in laser-quenched titanium alloys. Phys Rev Lett 54:2103
70. Yavari AR (2005) Solving the hume-rothery eutectic puzzle using miracle glasses. Nat Mater 4:1–2
71. Sudavtsova VS, Kotova NV (2009) Thermodynamic properties of binary Si–Y (transition metal) alloys powder metallurgy and metal ceramics, 48: 582-587. Translated from Poroshkovaya Metallurgiya 48:115–123
72. Senkov ON, Miracle DB (2001) Effect of the atomic size distribution on glass forming ability of amorphous metallic alloys. Mater Res Bull 36:2183–2198
73. Burlington MA (2004) Smithells metals reference book. In: Gale WF, Totemeier TC (eds) ASM international metals reference book, 8th edn. Elsevier Butterworth-Heinemann Ltd., Oxford UK, pp 4–44
74. Batsanov SS (1994) General and inorganic chemistry: metallic radii of nonmetals. Russ Chem Bull 43:199–201
75. Louzguine DV, Saito M, Waseda Y, Inoue A (1999) Structural study of amorphous $Ge_{50}Al_{40}Cr_{10}$ alloy. J Phys Soc Jpn 68:2298–2303
76. Botta WJ, Pereira FS, Bolfarini C, Kiminami CS, de Oliveira MF (2008) Topological instability and electronegativity effects on the glass-forming ability of metallic alloys. Philos Mag Lett 88:785–791
77. Yao KF, Chen N (2008) Pd–Si binary bulk metallic glass. Sci China Ser G 51:414–420
78. Chen N, Yang HA, Caron A, Chen PC, Lin YC, Louzguine-Luzgin DV, Yao KF, Esashi M, Inoue A (2011) Glass-forming ability and thermoplastic formability of a $Pd_{40}Ni_{40}Si_4P_{16}$ glassy alloy. J Mater Sci 46:2091–2096. doi:10.1007/s10853-010-5043-x
79. Louzguine DV, Inoue A (1999) The influence of cooling rate on the formation of an amorphous phase in Si-based multicomponent alloys and its thermal stability. Mater Res Bull 34:1165–1172
80. Bergman C, Chastel R, Gilbert M, Castanet R, Mathieu JC (1980) Short-range order and thermodynamic behaviour of Pd-Si melts. J Phys Colloques 41:591–594
81. Guo FQ, Poon SJ, Shiflet GJ (2004) CaAl-based bulk metallic glasses with high thermal stability. Appl Phys Lett 84:37–39
82. Mendeleev D (1889) The periodic law of the chemical elements. J Chem Soc 55:634–656
83. Winter M (2008) WebElements: the periodic table on the WWW, vol 2007. The University of Sheffield and WebElements Ltd, Sheffield
84. Nagel SR, Taue J (1975) Nearly-free-electron approach to the theory of metallic glass alloys. Phys Rev Lett 35:380
85. Hiiussler P (1983) Interrelations between electronic and ionic structure in metallic glasses. Z Phys B Cond Matt 53:15
86. Louzguine DV, Inoue A (2002) Investigation of structure and properties of the Al–Y–Ni–Co–Cu metallic glasses. J Mater Res 17:1014–1018
87. Louzguine-Luzgin DV, Inoue A (2005) Structure and transformation behaviour of a rapidly solidified Al–Y–Ni–Co–Pd alloy. J Alloys Compd 399:78–85
88. Perepezko JH, Hildal K (2008) Metallic glass formation reactions and interfaces. Mater Sci and Eng B 148:171–178
89. Perepezko JH, Imhoff SD, Hebert RJ (2010) Nanostructure development during devitrification and deformation. J Alloys Compd 495:360–364
90. Huang Z, Li J, Rao Q, Zhou Y (2008) Thermal stability and primary phase of Al–Ni(Cu)–La amorphous alloys. J Alloys Compd 463:328
91. Tkatch VI, Rassolov SG, Popov VV, Maksimov VV, Maslov VV, Nosenko VK, Aronin AS, Abrosimova GE, Rybchenko OG (2011) Complex crystallization mode of amorphous/nanocrystalline composite $Al_{86}Ni_2Co_{5.8}Gd_{5.7}Si_{0.5}$. J Non-Cryst Solids 357:163–1628
92. Wang H, Carter EA (1993) Metal-metal bonding in Engel-Brewer intermetallics: "anomalous" charge transfer in zirconium-platinum ($ZrPt_3$). J Am Chem Soc 115:2357–2362
93. Louzguine-Luzgin DV (2014) Vitrification and devitrification processes in metallic glasses. J Alloy Compd 586:S2–S8
94. Ojovan MI (2013) Ordering and structural changes at the glass–liquid transition. J Non-Cryst Solids 382:79–86
95. Senkov ON (2007) Correlation between fragility and glass-forming ability of metallic alloys. Phys Rev B 76:104202
96. Uhlmann DR (1972) A kinetic treatment of glass formation. J Non-Cryst Solids 7:337–348